Structural Analysis of NSAID Binding by Prostaglandin H_2 Synthase: Time-Dependent and Time-Independent Inhibitors Elicit Identical Enzyme Conformations†

Barry S. Selinsky,‡,§ Kushol Gupta,§,|| Caroline T. Sharkey,⊥ and Patrick J. Loll*,||

Department of Chemistry, Villanova University, Villanova, Pennsylvania 19085, Department of Pharmacology, University of Pennsylvania, Philadelphia, Pennsylvania 19104, and Department of Clinical Pharmacology, Royal College of Surgeons in Ireland, Dublin 2, Ireland

Received January 5, 2001

ABSTRACT: Nonsteroidal antiinflammatory drugs (NSAIDs) block prostanoid biosynthesis by inhibiting prostaglandin H_2 synthase (EC 1.14.99.1). NSAIDs are either rapidly reversible competitive inhibitors or slow tight-binding inhibitors of this enzyme. These different modes of inhibition correlate with clinically important differences in isoform selectivity. Hypotheses have been advanced to explain the different inhibition kinetics, but no structural data have been available to test them. We present here crystal structures of prostaglandin H_2 synthase-1 in complex with the inhibitors ibuprofen, methyl flurbiprofen, flurbiprofen, and alclofenac at resolutions ranging from 2.6 to 2.75 Å. These structures allow direct comparison of enzyme complexes with reversible competitive inhibitors (ibuprofen and methyl flurbiprofen) and slow tight-binding inhibitors (alclofenac and flurbiprofen). The four inhibitors bind to the same site and adopt similar conformations. In all four complexes, the enzyme structure is essentially unchanged, exhibiting only minimal differences in the inhibitor binding site. These results argue strongly against hypotheses that explain the difference between slow tight-binding and fast reversible competitive inhibition by invoking global conformational differences or different inhibitor binding sites. Instead, they suggest that the different apparent modes of NSAID binding may result from differences in the speed and efficiency with which inhibitors can perturb the hydrogen bonding network around Arg-120 and Tyr-355.

Prostaglandin H_2 synthase (COX)[1] catalyzes the first committed step in the conversion of arachidonic acid to prostaglandins (*1*, *2*). Prostaglandins contribute to a wide variety of both normal and pathological cellular processes, including inflammation, platelet aggregation, pyresis, and parturition. As a result, modulation of COX activity can have profound physiological consequences, and drugs which inhibit COX have proven to be of immense clinical importance (*3*). There are two known COX isoforms, the "housekeeping" form COX-1, which is constitutively expressed in a broad range of tissues, and the inducible proinflammatory form COX-2, which is found primarily at sites of inflammation, in tumors, and in the central nervous system. Both isoforms possess two distinct enzymatic activities: the cyclooxygenase activity, which oxygenates arachidonic acid to form prostaglandin G_2, and the peroxidase activity, which reduces prostaglandin G_2 to prostaglandin H_2.

COX is an integral membrane protein, and forms homodimers with a molecular mass of approximately 140 kDa. The X-ray crystal structure of the protein has revealed it to be a monotopic membrane protein (*4*, *5*). The cyclooxygenase active site is found in the protein's interior; it is connected to the membrane by a long nonpolar channel, by which the substrate arachidonic acid gains access (*6*). The peroxidase active site is spatially distinct from the cyclooxygenase channel, lying on the exterior of the protein, on the side of the molecule opposite from the membrane-binding domain.

The cyclooxygenase activity of COX is the target of nonsteroidal antiinflammatory drugs (NSAIDs) such as aspirin, ibuprofen, naproxen, and indomethacin. NSAIDs are among the most important drugs in common use, both economically and clinically. Much attention has recently been devoted to the development of COX-2 selective inhibitors such as celecoxib and rofecoxib. These selective inhibitors are expected to retain potent antiinflammatory activity but lack the gastric side effects associated with classical nonselective NSAIDs (*7*−*9*).

While all NSAIDs act by blocking prostaglandin biosynthesis through inhibition of COX, different drugs achieve this via different mechanisms. Some NSAIDs, such as ibuprofen and methyl flurbiprofen, are classical time-

† This work was supported from a grant from the National Institutes of Health (GM55171).

* To whom correspondence should be addressed: Department of Pharmacology, University of Pennsylvania, 3620 Hamilton Walk, Philadelphia, PA 19104-6084. Phone: (215) 898-1294. Fax: (215) 573-2236. E-mail: loll@pharm.med.upenn.edu.

‡ Villanova University.

§ These authors contributed equally to this work.

|| University of Pennsylvania.

⊥ Royal College of Surgeons in Ireland.

[1] Abbreviations: COX, cyclooxygenase [prostaglandin H_2 synthase (EC 1.14.99.1)]; EPR, electron paramagnetic resonance; NCS, noncrystallographic symmetry; NSAID, nonsteroidal antiinflammatory drug; rms, root-mean-square.

10.1021/bi010045s CCC: $20.00
Published on Web 04/04/2001

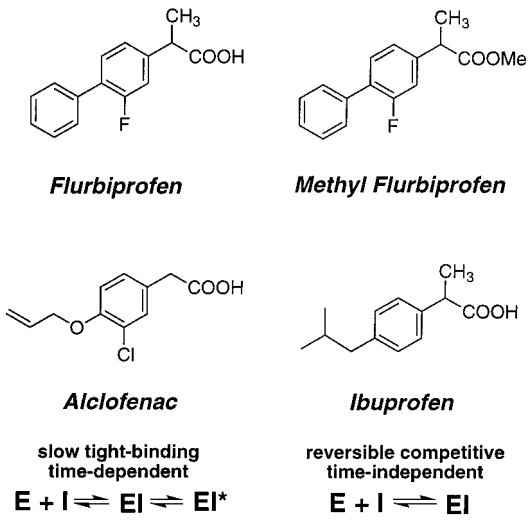

FIGURE 1: Inhibitors used in this study. Kinetic schemes are shown for both reversible competitive (time-independent) inhibition and slow tight-binding (time-dependent) inhibition.

independent competitive inhibitors which form reversible enzyme−inhibitor (EI) complexes (see Figure 1). Others, such as alclofenac and flurbiprofen, are time-dependent, slow tight-binding inhibitors that initially form a reversible EI complex, which is then gradually converted to an inactive form, termed EI* (*10*−*12*). Recent stopped-flow fluorescence measurements have suggested that these kinetic models may be oversimplified (*13*), but the general model of an initial bimolecular binding event, followed by one or more unimolecular steps, still seems to adequately describe time-dependent inhibition.

The difference between time-dependent and time-independent inhibition is clinically relevant, as it underlies the isoform-specific inhibition seen with selective COX-2 inhibitors (*14*−*16*). An understanding of the EI → EI* transition associated with time-dependent inhibition should therefore be useful in the rational design of novel therapeutics. Different hypotheses have been advanced to explain this phenomenon, including the invocation of a structural rearrangement between EI and EI* and the suggestion that time-dependent and time-independent inhibitors occupy distinct binding sites (*14*, *17*, *18*). To gain deeper insight into the mechanism of NSAID binding, we have determined X-ray crystal structures of the complexes of COX-1 with four chemically related inhibitors that are either reversible competitive inhibitors or slow tight-binding inhibitors (Figure 1). The structures reveal that the two types of inhibitors occupy the same binding site and adopt similar conformations, and that the enzyme conformation is invariant in all the complexes. These results suggest that time-dependent and time-independent NSAIDs may inhibit by similar mechanisms, and differ only in the speed and efficiency with which they can effect entry into their binding site.

EXPERIMENTAL PROCEDURES

Materials. Arachidonic acid was obtained from Cayman Chemicals (Ann Arbor, MI). Detergents were obtained from Anatrace (Maumee, OH), and ibuprofen and flurbiprofen were obtained from Sigma (St. Louis, MO). Alclofenac was a kind gift of Continental Pharma, Inc. (Brussels, Belgium). Other reagents and PEG-4000 were obtained from Aldrich Chemical Co. (Milwaukee, WI) and Fluka (Ronkonkoma, NY) and were of the highest quality commercially available.

Methyl Flurbiprofen. The methyl ester of flurbiprofen was prepared as follows. Flurbiprofen (1.0 g) was dissolved in 50 mL of methanol. Concentrated HCl (1 mL) was added and the reaction mixture stirred at room temperature overnight. Chloroform (25 mL) and water (50 mL) were added, with sufficient solid sodium carbonate to neutralize the HCl. The aqueous phase was extracted with an additional 25 mL of chloroform, and the combined chloroform phases were washed with 1% sodium carbonate and brine. The solution was dried and filtered, and the solvent was removed under vacuum to yield the final product (0.68 g, 64%). The product was homogeneous by silica thin-layer chromatography and NMR: ^{1}H NMR (300 MHz, $CDCl_3$) δ 1.53 (d, $J = 7.2$ Hz, 3H), 3.70 (s, 3H), 3.76 (quartet, $J = 7.2$ Hz, 1H); ^{13}C NMR (75 MHz, $CDCl_3$) δ 18.4, 44.9, 52.2, 115.2, 123.5, 127.7, 128.4, 129.0, 130.8, 135.5, 141.8, 159.7 (d, $J = 249$ Hz), 174.4.

Protein Purification and Crystallization. Ovine COX-1 was purified from ram seminal vesicles and crystallized essentially as described previously (*19*). To reduce the likelihood that crystal lattice contacts might lock the protein in any particular conformation, enzyme was dialyzed against 1 mM inhibitor solutions overnight, and then cocrystallized in the presence of inhibitor. This allowed ample time for equilibrium to be established and for the enzyme to arrive at its final structure [if it is assumed that the minimum time required to reach equilibrium is 10 times the half-life for the slowest kinetic step, then slow binding equilibrium will be achieved for flurbiprofen in <5 min (*20*)]. Thus, any structural rearrangements that might occur would already have taken place before crystal lattice contacts were formed. The dialysis buffer contained 20 mM sodium phosphate (pH 6.7), 50 mM NaCl, 0.6% (w/w) octyl glucopyranoside, and 1 mM inhibitor. In the case of methyl flurbiprofen, which displayed poor solubility in the aqueous buffers used here, the inhibitor was also included inside the dialysis bag. After dialysis, the protein solution was adjusted to 1.5−3% PEG-4000 and 50−125 mM NaCl and set up in hanging-drop vapor diffusion trays against 2−4-fold concentrated buffer containing 4−6.5% (w/w) PEG-4000. Crystallization experiments were carried out at 4 (ibuprofen) or 18 °C (flurbiprofen, alclofenac, and methyl flurbiprofen). Long brown rod-shaped crystals (0.5 mm × 0.1 mm × 0.1 mm) grew within 1−2 weeks. Crystals were harvested from the original mother liquor into cryoprotectant buffer containing 30% glycerol, 7.5% (w/w) PEG-4000, 15 mM sodium phosphate (pH 6.7), 113 mM NaCl, 0.4% (w/w) octyl glucopyranoside, 1 mM inhibitor, and 0.1 mM diethyldithiocarbamic acid using a five-step transfer, and were then immediately flash cooled in liquid nitrogen.

Crystal Dissolution Experiments. Approximately 10−15 large single crystals of the relevant inhibitor complex (flurbiprofen or ibuprofen) were harvested into buffers designed to mimic the original mother liquors, but which contained no inhibitor. The crystals were washed by two additional transfers into fresh aliquots of buffer, allowing 5 min for each wash step. Crystals were then dissolved in 50 μL of 0.1 M Tris (pH 8.0) and 0.6% octyl glucopyranoside. At various time points, aliquots of this solution were assayed

Table 1: Data Collection and Refinement Statistics

	ibuprofen	flurbiprofen	alclofenac	methyl flurbiprofen
		Data Collection		
resolution (Å)	2.61	2.70	2.69	2.75
total no. of observations	323752	273874	408172	217384
total no. of reflections	69417	60445	62943	53357
completeness				
overall (outer shell) (%)	90.9 (74.4)	97.3 (93.8)	98.2 (87.0)	88.2 (94.0)
R_{merge}				
overall (outer shell)	0.052 (0.187)	0.061 (0.193)	0.046 (0.125)	0.060 (0.189)
		Refinement		
R_{work}[a]	0.223	0.210	0.211	0.217
R_{free}[a]	0.250	0.242	0.242	0.252
rms deviation for bonds (Å)	0.007	0.007	0.008	0.008
rms deviation for angles (deg)	1.3	1.3	1.4	1.4
residues in the most preferred region of the Ramachandran diagram (%)	87.8	89.0	88.4	87.5
no. of water molecules	251	254	238	150
average *B*-value (Å^2)	24.7	23.2	24.9	38.4

[a] $R = \sum|F_{obs} - F_{calc}|/\sum|F_{obs}|$, where F_{obs} and F_{calc} are the observed and calculated structure factors, respectively. R_{free} was calculated using 7.5% of all reflections. The percentages of residues within the most preferred region of the Ramachandran diagram were determined by PROCHECK. The remainder of the residues in each model fall within the additionally allowed regions of the Ramachandran diagram.

for cyclooxygenase activity, using a coupled cyclooxygenase−peroxidase assay (*21*). Five microliters of the enzyme solution was added to a cuvette containing 96 mM Tris (pH 8.0), 8 μM hematin, and 76.8 μM TMPD in a final volume of 625 μL. The reaction was initiated by addition of 5 μL of a 3.3 mM solution of arachidonic acid, and oxidation of TMPD was monitored at 611 nm.

Data Collection. Data were collected at 100 K, using National Synchrotron Light Source beamlines X12B, X12C, and X8C. All inhibitor complex crystals belong to space group *I*222, with the following cell dimensions: $a = 98.65$ Å, $b = 204.99$ Å, and $c = 221.96$ Å (COX-1−ibuprofen), $a = 98.69$ Å, $b = 206.52$ Å, and $c = 220.34$ Å (COX-1−flurbiprofen), $a = 99.15$ Å, $b = 208.45$ Å, and $c = 222.40$ Å (COX-1−alclofenac), and $a = 98.89$ Å, $b = 209.5$ Å, and $c = 223.01$ Å (methyl flurbiprofen). The data were integrated and scaled using DENZO and SCALEPACK (*22*); details are given in Table 1.

Structure Solution and Refinement. Starting models for both enzyme−inhibitor complexes were derived from a 3.1 Å model of ovine COX-1 complexed to flurbiprofen (*23*). Initial positioning of a model including COX-1 residues 33−583 and the heme group was achieved by either rigid body refinement or molecular replacement followed by rigid body refinement, using the CNS program package (*24*). All models were then subjected to simulated annealing, *B*-value refinement, and conjugate gradient refinement using all available data. Missing features (inhibitors, carbohydrate, and detergent) were built into $F_o - F_c$ density, using the program O (*25*). Rebuilding and refinement were continued in an iterative manner. Water molecules having satisfactory $F_o - F_c$ density and good hydrogen bonding geometry were added to the model for additional refinement.

All structures were determined at similar resolutions from crystals grown under similar conditions; all have been refined to a similar degree and yield similar statistics (see Table 1). Because the starting models for these refinements were derived from the 3.1 Å structure of the COX-1 complex with the time-dependent inhibitor flurbiprofen (*23*), particular care was taken to ensure the structures were not biased toward the starting model, including the repeated use of simulated annealing omit maps (*26*).

The crystal asymmetric unit contains two identical COX-1 molecules related by a noncrystallographic 2-fold axis of symmetry. Refinement was performed initially with NCS constraints, and subsequently with tight NCS restraints, relaxing restraints in the inhibitor binding sites and at crystal contact points. The final models are of high quality, as assessed by the program PROCHECK (*27*); all have overall *G*-factors ranging from 0.27 to 0.31. Model statistics are listed in Table 1.

Accession Numbers. Atomic coordinates and structure factors have been deposited with the Protein Data Bank (entries 1HT8, 1EQH, 1EQG, and 1HT5 for the alclofenac, flurbiprofen, ibuprofen, and methyl flurbiprofen complexes, respectively).

RESULTS

Comparison of the Four Inhibitor Structures. The four structures presented here are the highest-resolution COX-1 structures currently available, and provide a significantly greater level of detail than previously published structures. The protein backbones of all four complexes are identical to within the expected error of the experiment, demonstrating that there is no global conformational difference between the EI and EI* complexes. Superposition yields overall rms differences of 0.15−0.36 Å for Cα positions and 0.37−0.48 Å for all atoms (see Table 2). By comparison, overall levels of coordinate error estimated from cross-validated Luzzati plots and sigmaA plots range from 0.32 to 0.38 Å (*28*). The variation of *B*-values with residue number is similar for all structures, indicating similar relative mobilities for different parts of the polypeptide chain (data not shown). Specific sites which have been suggested to play roles in time-dependent inhibition, including Arg-277 and Gln-358 (*29*), Arg-120 (*30*), Tyr-355 (*18*), Ile-523 (*31*, *32*), and residues 106−123 (*33*), directly overlie one another when the four structures are superimposed. Water structure in the vicinity of the inhibitors is similar in the four complexes, with every water

Table 2: Superposition of the Four COX-1−NSAID Complex Structures[a]

	flurbiprofen	methyl flurbiprofen	alclofenac	ibuprofen
flurbiprofen	−	*0.36*	*0.27*	*0.15*
methyl flurbiprofen	0.45	−	*0.19*	*0.35*
alclofenac	0.46	0.44	−	*0.26*
ibuprofen	0.37	0.48	0.43	−

[a] Pairwise rms differences in atomic positions are given in angstroms. The numbers in italics shown in the upper half of the matrix show superposition results for α-carbons only; the numbers in the lower half of the matrix show superposition results for all atoms.

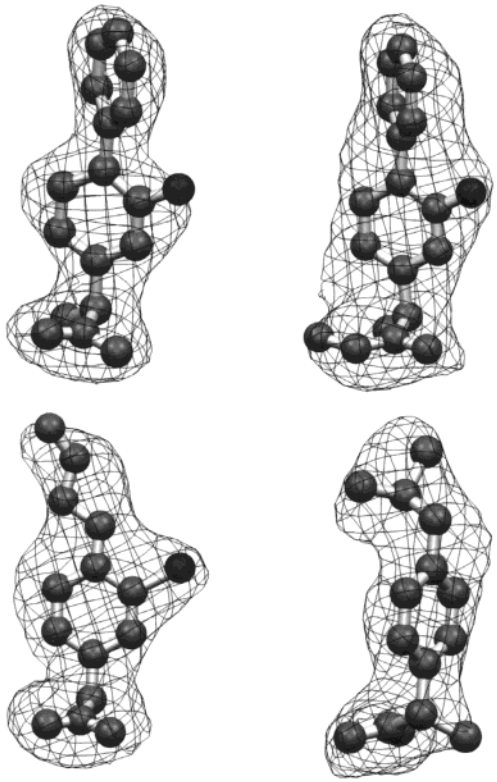

FIGURE 2: Simulated annealing omit electron density for each of the four inhibitors when bound in the COX active site: (top left) flurbiprofen, (top right) methyl flurbiprofen, (bottom left) alclofenac, and (bottom right) ibuprofen. SA omit calculations were performed after removing inhibitors and any nearby water molecules from the models. Maps are contoured at three standard deviations. This figure was made with the program SETOR (*49*).

site within 8 Å of the ligand being occupied at significant levels in all structures. Hence, binding or expulsion of a water molecule is also unlikely to account for the difference between time-dependent and time-independent inhibitor binding.

General Features of Inhibitor Binding. The four inhibitors bind in the cyclooxygenase active site, which lies at the apex of a long narrow hydrophobic channel extending from the membrane-binding surface to the center of the protein (*5*). The electron density for all four inhibitors is clear and well-defined (Figure 2). The four inhibitors that were studied share a common phenylacetic acid core structure (Figure 1). The carboxylate ends of these molecules differ in whether the carboxylic acid is free or blocked, and by the presence or absence of an α-methyl group. Despite these differences, the carboxylate groups of the inhibitors are essentially superimposable (see Figure 3). The inhibitor carboxylates take part in a network of polar interactions which includes two hydrogen bonds between the inhibitor and Arg-120, salt bridges between Arg-120 and Glu-524, and hydrogen bonds between the inhibitors, the phenolic hydroxyl of Tyr-355, and at least two well-ordered water molecules (Figure 4). Methylation of the carboxylate causes only a slight perturbation in inhibitor positioning, which is necessary to relieve a close contact between the methyl group and the side chain of Leu-531. This is achieved by a small rotation about the bond connecting the first phenyl ring to the α-carbon of the inhibitor, and all of the specific interactions made between the carboxylate group and the protein are preserved in the methyl flurbiprofen complex.

The amino acid side chains that lie near the carboxylate groups of the inhibitors (His-90, Arg-120, Tyr-355, and Glu-524) mesh together to form a constriction in the active site channel that tightly locks the inhibitor into place. It has been proposed that the slow step of slow tight-binding inhibition involves a rearrangement or disruption of the hydrogen bonding network around these side chains, and that a comparable disruption does not occur with time-independent inhibitors (*18*). However, the crystal structures demonstrate that this hydrogen bond network is conserved between the time-dependent and time-independent inhibitor complexes. In addition, no clear solvent channel connects the inhibitors with the outside of the enzyme, indicating that some protein conformational change is required to allow either type of inhibitor to enter or exit the active site.

The most substantial differences between the four inhibitors are found in the substituents on the phenyl ring, which lie at the end of the molecule opposite (distal) from the carboxylic acid group. The distal regions of the inhibitors lie in a hydrophobic cavity lined by Leu-352, Tyr-385, Trp-387, Tyr-348, Phe-518, Gly-526, and Ser-530. This cavity is somewhat larger than the ligands. As a consequence, none of the atoms in the distal end of the ibuprofen molecule are actually in van der Waals contact with the enzyme. Flurbiprofen, methyl flurbiprofen, and alclofenac are slightly larger than ibuprofen, and the atoms at the extreme distal end of these molecules do make van der Waals contact with protein residues; however, the atoms in the middle part of the inhibitors do not contact any protein atoms.

The distal portions of flurbiprofen and methyl flurbiprofen are identical, and they occupy exactly the same position in the channel (Figure 3). The fluorine atom found on the first phenyl ring protrudes into a hydrophobic cleft lined by the side chains of Leu-352, Phe-518, and Ile-523. The second phenyl ring lies alongside the side chains of Leu-352 and Ser-530 and next to the protein backbone at Gly-522; above this phenyl ring lies the "roof" of the cyclooxygenase active site, formed by the side chains of Phe-381, Leu-384, Tyr-385, and Trp-387.

Ibuprofen contains an isobutyl substituent on its phenyl ring, rather than a second aromatic group; also, it is not halogenated. Its phenyl ring is rotated slightly toward Val-349, relative to those of the other inhibitors. Ibuprofen's isobutyl group occupies the same position in the cyclooxygenase channel as the second phenyl rings of flurbiprofen and methyl flurbiprofen. However, in contrast to flurbiprofen and methyl flurbiprofen, the only close contacts made between the enzyme and ibuprofen are in the propionic acid

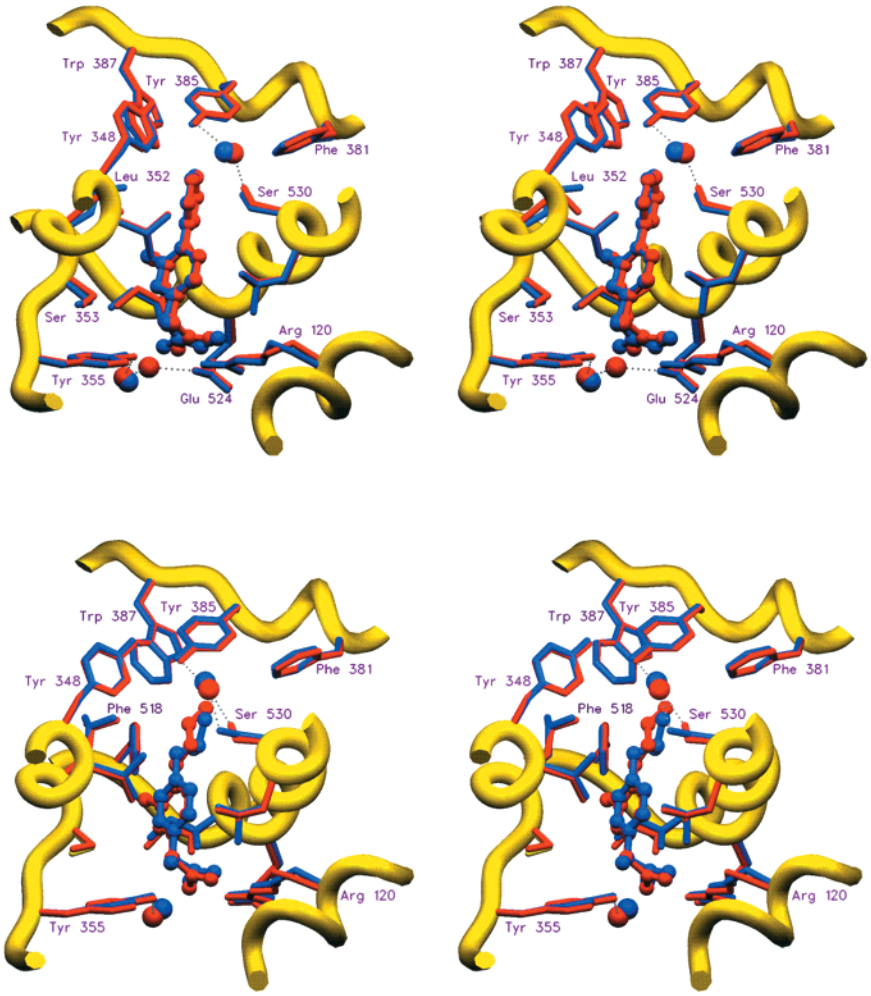

FIGURE 3: Divergent stereoviews of the cyclooxygenase active site. The top panel shows the superposition of the flurbiprofen and the methyl flurbiprofen complexes; the bottom panel shows the superposition of the alclofenac and ibuprofen complexes. Inhibitors are shown in ball-and-stick representations. In both panels, the complex with the slow tight-binding inhibitor is shown in red while the complex with the reversible competitive inhibitor is shown in blue. Hence, in the top panel flurbiprofen is red and methyl flurbiprofen blue and in the bottom panel alclofenac is red and ibuprofen blue. Several conserved water molecules are shown as isolated spheres, along with their inferred hydrogen bonding patterns (dashed lines). This figure was made with the program SETOR (*49*).

region of the molecule and the parts of the ring closest to the propionic acid; the distal portion of the ring and the isobutyl group are all at least 3.7 Å away from the nearest protein atoms.

Alclofenac lacks an α-methyl substituent on its phenyl acetic acid structure, allowing the α-carbon to move slightly closer to Leu-359 than is possible for the other three inhibitors. This causes alclofenac's phenyl ring to be cocked slightly relative to those of the other inhibitors. As a result, the chlorine atom is inserted more deeply into the cleft formed by Leu-352, Phe-518, and Ile-523 than are the fluorine atoms in flurbiprofen and methyl flurbiprofen. In addition, the slight rotation of the alclofenac phenyl ring appears to aid in accommodating the allyloxy substituent at the top of the cyclooxygenase pocket. The three allylic carbons of the inhibitor lie within van der Waals distance of Trp-387 and Ser-530; however, the distance from the ether oxygen to the nearest protein atom is greater than 4 Å.

The differences in positioning of the four inhibitors are subtle, and the enzyme is able to accommodate them with only small changes in the positions of the Leu-352 and Ser-530 side chains (Figure 3). The fact that the cyclooxygenase cavity is larger than required to contain the inhibitors implies that considerable variation in inhibitor structure could be accommodated without changing the protein conformation. While it might seem that better NSAID binding could be achieved by increasing the size of the inhibitor to match the size of the cavity, it is possible that larger inhibitors would be unable to negotiate the lower reaches of the cyclooxygenase channel. Thus, the maximum inhibitor size may be determined by what can pass through the Arg-120−Tyr-355 constriction.

The side chain of Ser-530 lies close to the distal phenyl ring of flurbiprofen, as has previously been described for both the COX-1 and COX-2 complexes (*5*, *33*), and a similar positioning is observed for methyl flurbiprofen. The distance from the oxygen to the center of the aromatic ring is 3.4 Å, appropriate for a hydroxyl−aromatic hydrogen bond (*34*−*36*). Ibuprofen lacks a hydrogen bond donor or acceptor in its distal portion, and does not form any specific interaction with Ser-530; as a consequence, Ser-530 adopts different rotomeric states in the ibuprofen and flurbiprofen structures. While alclofenac does contain an oxygen atom that could conceivably hydrogen bond with Ser-530, an unfavorable positioning of the allylic group precludes formation of such a bond. Model building suggests that any conformational

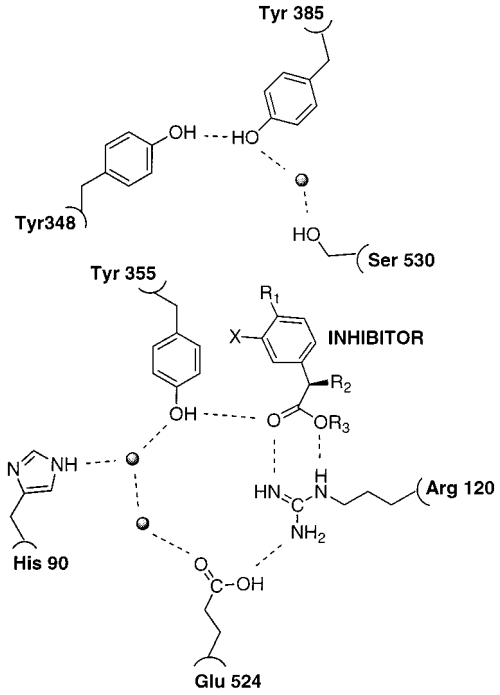

FIGURE 4: Schematic representation of key polar interactions in the cyclooxygenase active site. The identities of the various substituents on the inhibitor molecules (R_1-R_3 and X) are given in Figure 1. Water molecules are shown as gray spheres.

change of the allylic group that might allow the ether oxygen to accept a hydrogen bond from Ser-530 would lead to unfavorable packing at the top of the cyclooxygenase channel and/or close contacts between the chlorine atom and the allylic group.

Well-ordered water molecules can be identified in the cyclooxygenase channels of all four inhibitor complex structures (Figure 4). One such molecule bridges the phenolic hydroxyl of Tyr-355 and the side chain of His-90. This water is hydrogen bonded to a second water, which in turn hydrogen bonds to Glu-524. These waters are seen in all four structures, and appear to play key roles in maintaining the structural integrity of the constriction in the cyclooxygenase channel.

An additional well-ordered water molecule is observed in all four structures at the top of the cyclooxygenase channel, where it forms hydrogen bonds with Ser-530 and Tyr-385. No catalytic role for this water molecule is immediately apparent, since the tyrosyl radical form of Tyr-385 is thought to be responsible for abstracting a hydrogen atom from the substrate (*37*). However, it is possible this water may assist in maintaining the native structure of the enzyme in the absence of substrate. Since Tyr-385 and Ser-530 lie in an extremely hydrophobic environment, electrostatic interactions such as hydrogen bonds are expected to take on great importance. This bridging water molecule would satisfy the hydrogen bonding capability of both residues, and yet still be capable of being displaced by substrate to allow Tyr-385 to perform its catalytic role. Consistent with this notion, the water molecule lies next to an alcove that branches off from the top of the cyclooxygenase channel, which is connected to the outside of the protein by a narrow solvent channel. This channel has been suggested to serve as a safety valve, allowing water to escape from the top of the cyclooxygenase active site as substrate enters from the bottom (*38*). The

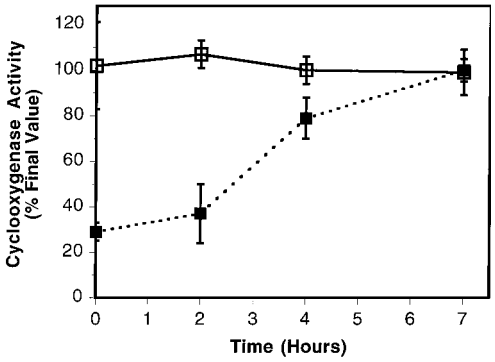

FIGURE 5: Time course of the recovery of cyclooxygenase activity from dissolved crystals of COX−NSAID complexes: (□) ibuprofen and (■) flurbiprofen. Mean values for each point and their associated standard errors were calculated from five different assays, representing three independent crystal dissolution experiments.

S530A mutant of COX retains cyclooxygenase activity, indicating that the bridging water is not essential for catalysis (*39*); however, since a detailed characterization of the kinetic and stability properties of this mutant is not available, the precise extent to which this water may contribute to catalysis and/or stability cannot be estimated. It is interesting to note that recent mutagenesis studies have revealed that the hydrogen bonding network in the vicinity of Tyr-385 is critical for the acetylation of Ser-530 by aspirin, and have suggested that Tyr-385 positions the acetyl group in the same position as this bridging water prior to nucleophilic attack by the serine hydroxyl (*40*).

Recovery of Activity from Dissolved Crystals. It is important to assess whether the similarity of the four structures reported here results from an artifact of crystallization. It is assumed that the complexes of COX with flurbiprofen and alclofenac represent the EI* state, and that the complexes with ibuprofen and methyl flurbiprofen reflect the EI state. However, it is possible that crystal packing forces have driven the ibuprofen and methyl flurbiprofen complexes into the EI* state. Since the EI* state is not normally observed in solution for time-independent inhibitors, the activation energy for the EI ↔ EI* transition for these inhibitors is either very low or very high. If it is low, then the EI ↔ EI* transition would be kinetically invisible, and one would expect the EI* state to be well-populated (this possibility is considered further in the Discussion). If the activation energy is high, then the EI → EI* transition would not normally occur, and the EI* state would not be populated to any appreciable extent. However, if crystal packing preferentially favors the EI* state, then the free energy associated with crystal lattice formation might be sufficient to drive a time-independent inhibitor complex from the EI state into the EI* state. To test for this possibility, crystals of the ibuprofen and flurbiprofen complexes were washed to remove excess inhibitor and then dissolved, and enzyme activity was measured over a period of hours following dissolution. For the ibuprofen complex, full enzyme activity was recovered immediately upon dissolving the crystals; however, the flurbiprofen complex required many hours to regain activity (see Figure 5). This is consistent with the flurbiprofen complex crystallizing as the EI* state, while the ibuprofen complex crystallizes as the EI state. If crystallization preferentially captured the EI* state, then both complexes would require a long time to recover activity. Indeed,

according to the hypothetical scenario described above, the ibuprofen complex should require more time to recover than the flurbiprofen complex, because of its higher transition energy. The essentially instantaneous recovery of activity from the ibuprofen complex proves that an EI* complex of ibuprofen has not been formed as an artifact of crystallization (or that for ibuprofen, no large barrier separates EI and EI*).

This result is consistent with the observation that crystal packing forces are more likely to select among conformers that occur in solution than to distort proteins into conformations not found in solution (*41*). In any event, forces contributed by lattice contacts are expected to be weak and to act at the molecule's surface; it would be surprising if such forces were able to trigger the same precise conformational changes as time-dependent inhibitors, which bind strongly to a site deep within the interior of the enzyme.

DISCUSSION

Nature of Slow Tight-Binding Inhibition. The slow equilibrium between EI and EI* observed with slow tight-binding inhibitors implies a large transition state barrier separating the two states; this barrier has been estimated to be approximately 18 kcal/mol for flurbiprofen binding to COX-1 (*20*). Given the important contributions of slow tight-binding inhibition to isoform specificity and potency, it is of interest to understand the nature of the EI $\rightarrow$ EI* rearrangement, and how the binding of slow tight-binding inhibitors differs from that of classical time-independent inhibitors.

A number of distinct hypotheses can be advanced to explain the nature of the slow tight-binding COX inhibition observed with many NSAIDs. We shall consider these hypotheses in light of our structural data.

Hypothesis 1: "Time-independent" inhibitors do not follow a simple E + I $\leftrightarrow$ EI binding mechanism. Instead, both time-dependent and time-independent inhibitors bind by the same E + I $\leftrightarrow$ EI $\leftrightarrow$ EI mechanism, and differ only in the energy of the EI $\leftrightarrow$ EI* transition*. Slow tight-binding inhibitors can only be experimentally identified because the equilibrium between EI and EI* is slow relative to catalysis (*18*). If the transition energy separating EI and EI* is low, then the transition will be rapid relative to catalysis and therefore kinetically invisible. Hence, it is possible that time-independent inhibitors do not follow the simple E + I $\leftrightarrow$ EI kinetic scheme shown in Figure 1. Rather, they could follow the same pathway for binding as slow tight-binding inhibitors do, and differ only insofar that the EI $\leftrightarrow$ EI* transition is rapid. If this hypothesis is correct, one would predict the crystal structure determination to reveal COX in the EI* state whether a slow tight-binding or a reversible competitive inhibitor is bound. The enzyme appears to have adopted the same conformational state for all four different inhibitors studied here, and the structural results are therefore in good agreement with this hypothesis.

According to this model, the binding of time-dependent and time-independent inhibitors is likely to differ in the EI state, and not in the EI* state. The precise nature of this difference, however, is not clear. One possibility is that time-dependent inhibitors form transient interactions with the lower portion of the cyclooxygenase channel; this would correspond to the EI state. These interactions would delay formation of EI* and be responsible for the high transition barrier that is observed. Only one NSAID binding site is observed in the crystal structures, so a conformational change may occur upon EI* formation that eliminates the transient EI site. Support for this model comes from recent fluorescence studies of holo-COX-2, which suggest that for a time-dependent inhibitor, EI and EI* correspond to inhibitor binding at distinct sites (*13*).

The question of why some inhibitors are delayed in the EI state, while others move quickly to the EI* state, remains to be answered. The kinetic differences between the two types of inhibitors may reflect differences in the efficiency with which they perturb the hydrogen bonding network in the vicinity of Arg-120 and Tyr-355.

Hypothesis 2: The EI $\rightarrow$ EI transition corresponds to a conformational rearrangement of the enzyme.* The possibility that the slow step in inhibition by NSAIDs such as flurbiprofen and alclofenac reflects an enzyme conformational change has been recognized by many laboratories (*11*, *14*, *20*, *29*). Factors rendering this possibility plausible include the size of the transition state barrier, the known conformational heterogeneity of COX (*42*, *43*), and structural changes accompanying slow tight-binding inhibition in other enzyme systems (*44*, *45*). Additionally, EPR studies of nitroxide-labeled COX-2 have suggested that binding of NSAIDs or substrate induces conformational changes in the enzyme (*46*). However, the crystal structures reported here show that no significant conformational change separates EI and EI*, and therefore, this hypothesis is not correct. Similar results have been observed with α-lytic protease and chymotrypsin (*47*, *48*). It is of course possible that a conformational change does occur, but is too subtle to be detected in these structures. Indeed, the difference between the ground state energies of EI and EI* is estimated to be only 0.6 kcal/mol for flurbiprofen (*20*). However, the large energy barrier associated with the EI $\rightarrow$ EI* transition does not appear to be consistent with the interconversion of two virtually identical structures.

Rejection of this hypothesis assumes that the COX−ibuprofen and COX−methyl flurbiprofen complex structures accurately reflect the EI state, and not the EI* state. If this is not true, than either the EI $\leftrightarrow$ EI* transition energy is low (which corresponds to hypothesis 1, above) or the EI $\leftrightarrow$ EI* transition energy is high, in which case the structural similarity of the four inhibitor complexes would reflect an artifact of crystallization. The second possibility is ruled out by the demonstration that enzymatic activity is recovered instantaneously upon dissolving crystals of the ibuprofen complex, but not the flurbiprofen complex, showing that the ibuprofen complex crystallizes as the EI state, and the flurbiprofen complex crystallizes as the EI* state.

Hypothesis 3: EI and EI represent inhibitor binding at two distinct sites.* The long narrow character of the cyclooxygenase channel means that different inhibitors might bind at different points along the channel, and yet block enzyme activity equally well. Therefore, it is possible that the EI state corresponds to inhibitor binding at one site, while the EI* state represents binding in a distinct site. According to this hypothesis, time-independent inhibitors would bind reversibly at the EI site. Time-dependent inhibitors would also bind reversibly at the EI site; after this initial binding, however, they would move to a second (EI*) site. In the context of the COX structure, it is reasonable to speculate

that the EI site would lie near the mouth of the cyclooxygenase channel, and that the transition to EI* would involve opening of the constriction around Arg-120 and Tyr-355 and movement of the inhibitor into the active site (*17*). Our data do not favor this hypothesis, since all inhibitors occupy precisely the same site. In addition, no evidence is observed for inhibitor binding at a second site elsewhere on the enzyme, despite the presence of a large excess of inhibitor in the crystallization experiment.

Hypothesis 4: The EI → EI transition involves conformational rearrangements of the inhibitor only, and not of the enzyme*. It is possible that the transition between EI and EI* involves no enzyme conformational change, but requires only motions of the inhibitor that lock it into place (e.g., reorientation of the two phenyl rings in flurbiprofen). Because the hydrophobic cavity in which NSAIDs bind is somewhat larger than the compounds themselves, inhibitors may still undergo ring flips and other movements after binding. However, since the cavity is only slightly larger than the inhibitors, such motions are likely to take place more slowly than in free solution, which could explain the relatively deliberate kinetics of EI* formation. This hypothesis would require that time-dependent inhibitors adopt one particular conformation to enter the active site, and then, after their arrival, isomerize to a different conformation that is not capable of exiting; the EI → EI* transition would correspond to this slow isomerization.

Our structural data, and in particular the structures of the flurbiprofen and methyl flurbiprofen complexes, argue against this hypothesis as well. Conversion of the time-dependent inhibitor flurbiprofen into its methyl ester changes it to a time-independent inhibitor (*12*). When refining the structures of the flurbiprofen and methyl flurbiprofen complexes, we took particular care to assign the positions of the fluorine atoms, to address the question of whether a ring flip separated the EI and EI* states. Simulated annealing omit maps unambiguously revealed that the fluorine atoms occupied the same position in both inhibitor complex structures (data not shown). The conformations of the two drugs in the COX active site are essentially identical.

Conclusions. This study shows that COX-1 adopts the same structure whether bound to slow tight-binding inhibitors or reversible competitive inhibitors, and that the two different types of inhibitors utilize the same binding site and adopt similar conformations. These results rule out several hypotheses that have been advanced to explain the different kinds of kinetic behavior. They also suggest a new model wherein reversible competitive inhibitors and slow tight-binding inhibitors bind and inhibit COX by the same mechanism, and differ principally in the speed and efficiency with which they can open the cyclooxygenase channel and gain access to the enzyme active site.

ACKNOWLEDGMENT

Diffraction data for this study were collected at Brookhaven National Laboratory in the Biology Department single-crystal diffraction facility at beamlines X12B, X12C, and X8C in the National Synchrotron Light Source. This facility is supported by the United States Department of Energy Offices of Health and Environmental Research and of Basic Energy Sciences, by the NSF, and by the NIH.

REFERENCES

1. Vane, J. R., Bakhle, Y. S., and Botting, R. M. (1998) *Annu. Rev. Pharmacol. Toxicol. 38*, 97−120.
2. Smith, W. L., DeWitt, D. L., and Garavito, R. M. (2000) *Annu. Rev. Biochem. 69*, 145−182.
3. Vane, J. R., and Botting, R. M. (1998) *Inflammation Res. 47* (Suppl. 2), S78−S87.
4. Picot, D., and Garavito, R. M. (1994) *FEBS Lett. 346*, 21−25.
5. Picot, D., Loll, P. J., and Garavito, R. M. (1994) *Nature 367*, 243−249.
6. Malkowski, M. G., Ginell, S. L., Smith, W. L., and Garavito, R. M. (2000) *Science 289*, 1933−1937.
7. Warner, T. D., Giuliano, F., Vojnovic, I., Bukasa, A., Mitchell, J. A., and Vane, J. R. (1999) *Proc. Natl. Acad. Sci. U.S.A. 96*, 7563−7568.
8. Marnett, L. J., and Kalgutkar, A. S. (1999) *Trends Pharmacol. Sci. 20*, 465−469.
9. Vane, J. R. (1995) *Lancet 346*, 1105−1106.
10. Morrison, J. F., and Walsh, C. T. (1988) *Adv. Enzymol. Relat. Areas Mol. Biol. 61*, 201−301.
11. Kulmacz, R. J., and Lands, W. E. M. (1985) *J. Biol. Chem. 260*, 12572−12578.
12. Rome, L. H., and Lands, W. E. M. (1975) *Proc. Natl. Acad. Sci. U.S.A. 72*, 4863−4865.
13. Lanzo, C. A., Sutin, J., Rowlinson, S., Talley, J., and Marnett, L. J. (2000) *Biochemistry 39*, 6228−6234.
14. Copeland, R. A., Williams, J. M., Biannaras, J., Nurnberg, S., Covington, M., Pinto, D., Pick, S., and Trzaskos, J. M. (1994) *Proc. Natl. Acad. Sci. U.S.A. 91*, 11202−11206.
15. Oellet, M., and Percival, M. D. (1995) *Biochem. J. 306*, 247−251.
16. Gierse, J. K., Koboldt, C. M., Walker, M. C., Seibert, K., and Isakson, P. C. (1999) *Biochem. J. 339*, 607−614.
17. Llorens, O., Perez, J. J., Palomer, A., and Mauleon, D. (1999) *Bioorg. Med. Chem. Lett. 9*, 2779−2784.
18. So, O. Y., Scarafia, L. E., Mak, A. Y., Callan, O. H., and Swinney, D. C. (1998) *J. Biol. Chem. 273*, 5801−5807.
19. Loll, P. J., Picot, D., Ekabo, O., and Garavito, R. M. (1996) *Biochemistry 35*, 7330−7340.
20. Callan, O. H., So, O. Y., and Swinney, D. C. (1996) *J. Biol. Chem. 271*, 3548−3554.
21. Kulmacz, R. J., and Lands, W. E. M. (1987) in *Prostaglandins and Related Substances, A Practical Approach* (Benedetto, C., McDonald-Gibson, R. G., Nigam, S., and Slater, T. F., Eds.) pp 209−227, IRL Press, Washington, DC.
22. Otwinowski, Z., and Minor, W. (1997) *Methods Enzymol. 276*, 307−326.
23. Garavito, R. M., Picot, D., and Loll, P. J. (1995) *Adv. Prostaglandin, Thromboxane, Leukotriene Res. 23*, 99−103.
24. Brunger, A. T., Adams, P. D., Clore, G. M., DeLano, W. L., Gros, P., Grosse-Kunstleve, W., Jiang, J. S., Kuszewski, J., Nilges, M., Pannu, N. S., Read, R. J., Rice, L. M., Simonson, T., and Warren, G. L. (1998) *Acta Crystallogr. D54*, 905−921.
25. Jones, T. A., and Kjeldgaard, M. (1997) *Methods Enzymol. 277*, 173−208.
26. Hodel, A., Kim, S. H., and Brunger, A. T. (1992) *Acta Crystallogr. A48*, 851−859.
27. Laskowski, R. A., MacArthur, M. W., Moss, D. S., and Thornton, J. M. (1993) *J. Appl. Crystallogr. 26*, 283−291.
28. Brunger, A. T. (1997) *Methods Enzymol. 277*, 366−396.
29. Pouplana, R., Perez, C., Sanchez, J., Lozano, J. J., and Puig-Parellada, P. (1999) *J. Comput.-Aided Mol. Des. 13*, 297−313.
30. Bhattacharyya, D. K., Lecomte, M., Rieke, C. J., Garavito, R. M., and Smith, W. L. (1996) *J. Biol. Chem. 271*, 2179−2184.
31. Wong, E., Bayly, C., Waterman, H. L., Riendeau, D., and Mancini, J. A. (1997) *J. Biol. Chem. 272*, 9280−9286.
32. Guo, Q., Wang, L. H., Ruan, K. H., and Kulmacz, R. J. (1996) *J. Biol. Chem. 271*, 19134−19139.
33. Kurumbail, R. G., Stevens, A. M., Gierse, J. K., McDonald, J. J., Stegeman, R. A., Pak, J. Y., Gildehaus, D., Miyashiro,

J. M., Penning, T. D., Seibert, K., Isakson, P. C., and Stallings, W. C. (1996) *Nature 384*, 644−648.
34. Cowan, S. W., Newcomer, M. E., and Jones, T. A. (1993) *J. Mol. Biol. 230*, 1225−1246.
35. Dobrowolski, J. C., and Jamroz, M. H. (1993) *J. Mol. Struct. 293*, 147−150.
36. Suzuki, S., Green, P. G., Bumgarner, R. E., Dasgupta, S., Goddard, W. A. I., and Blake, G. A. (1992) *Science 257*, 942−945.
37. Smith, W. L., Eling, T. E., Kulmacz, R. J., Marnett, L. J., and Tsai, A. (1992) *Biochemistry 31*, 3−7.
38. Picot, D. (1998) in *Eicosanoids, Aspirin, and Asthma* (Szczeklik, A., Gryglexski, R. J., and Vane, J. R., Eds.) pp 161−186, Marcel Dekker, New York.
39. DeWitt, D. L., El-Harith, A., Kraemer, S. A., Andrews, M. J., Yao, E. F., Armstrong, R. L., and Smith, W. L. (1990) *J. Biol. Chem. 265*, 5192−5198.
40. Hochgesang, G. P. J., Rowlinson, S. W., and Marnett, L. J. (2000) *J. Am. Chem. Soc. 122*, 6514−6515.
41. Kossiakoff, A. A., Randal, M., Guenot, J., and Eigenbrot, C. (1992) *Proteins 14*, 65−74.
42. Kulmacz, R. J. (1989) *J. Biol. Chem. 264*, 14136−14144.
43. Luong, C., Miller, A., Barnett, J., Chow, J., Ramesha, C., and Browner, M. F. (1996) *Nat. Struct. Biol. 3*, 927−933.
44. Bonneau, P., Grand-Maitre, C., Greenwood, D. J., Lagace, L., La Plante, S. R., Massariol, M. J., Ogilvie, W. W., O'Meara, J. A., and Kawai, S. (1997) *Biochemistry 36*, 12644−12652.
45. Betz, A., Wong, P. W., and Sinhu, U. (1999) *Biochemistry 38*, 14582−14591.
46. Smith, T., McCracken, J., Shin, Y. K., and DeWitt, D. (2000) *J. Biol. Chem. 275*, 40407−40415.
47. Bone, R., Frank, D., Kettner, C. A., and Agard, D. A. (1989) *Biochemistry 28*, 7600−7609.
48. Brady, K., Wei, A. Z., Ringe, D., and Abeles, R. H. (1990) *Biochemistry 29*, 7600−7607.
49. Evans, S. V. (1993) *J. Mol. Graphics 11*, 134−138.

BI010045S